Title
Diesel Exhaust Induces Mitochondrial Dysfunction, Hyperlipidemia, and Liver Steatosis.

Journal
Arteriosclerosis, thrombosis, and vascular biology, 39(9)

ISSN
1079-5642

Authors
Yin, Fen
Gupta, Rajat
Vergnes, Laurent
et al.

Publication Date
2019-09-01

DOI
10.1161/atvbaha.119.312736

Peer reviewed

HHS Public Access

Author manuscript

Arterioscler Thromb Vasc Biol. Author manuscript; available in PMC 2020 September 01.

Published in final edited form as:

Arterioscler Thromb Vasc Biol. 2019 September ; 39(9): 1776–1786. doi:10.1161/ATVBAHA.119.312736.

Diesel Exhaust Induces Mitochondrial Dysfunction, Hyperlipidemia and Liver Steatosis

Fen Yin[1], **Rajat Gupta**[1], **Laurent Vergnes**[2], **Will S. Driscoll**[3], **Jerry Ricks**[3], **Gajalakshmi Ramanathan**[1], **James A. Stewart**[4], **Diana M. Shih**[1], **Kym F. Faull**[5], **Simon W. Beaven**[6], **Aldons J. Lusis**[1,2], **Karen Reue**[2], **Michael E. Rosenfeld**[3,4], **Jesus A. Araujo**[1,7]

[1]Division of Cardiology, David Geffen School of Medicine at University of California Los Angeles, 10833 Le Conte Avenue, CHS 43-264, Los Angeles, CA

[2]Department of Human Genetics, David Geffen School of Medicine at University of California Los Angeles, 659 Charles E. Young Drive South, Los Angeles, CA

[3]Department of Pathology, University of Washington, Seattle, WA

[4]Department of Environmental and Occupational Health Sciences, University of Washington, Seattle, WA

[5]Pasarow Mass Spectrometry Laboratory, Semel Institute for Neuroscience and Human Behavior and Department of Psychiatry and Biobehavioral Sciences, David Geffen School of Medicine at University of California Los Angeles, 760 Westwood Boulevard, Los Angeles, CA

[6]Division of Gastroenterology, David Geffen School of Medicine at University of California Los Angeles, 10833 Le Conte Avenue, CHS 44-144, Los Angeles, CA

[7]Department of Environmental Health Sciences, Fielding School of Public Health, University of California Los Angeles, 10833 Le Conte Avenue, CHS 43-264, Los Angeles, CA

Abstract

Objective: Air pollution is associated with increased cardiovascular morbidity and mortality as well as dyslipidemia and metabolic syndrome. Our goal was to dissect the mechanisms involved.

Approach and Results: We assessed the effects of exposure to air pollution on lipid metabolism in mice through assessment of plasma lipids and lipoproteins, oxidized fatty acids 9-HODE and 13-HODE, lipid and carbohydrate metabolism. Findings were corroborated and mechanisms were further assessed in HepG2 hepatocytes in culture. ApoE KO mice exposed to inhaled diesel exhaust (DE, 6 hours/day, 5 days/week for 16 weeks) exhibited elevated plasma cholesterol and triglyceride levels, increased hepatic triglyceride content and higher hepatic levels of 9-HODE and 13-HODE, as compared with control mice exposed to filtered air (FA). A direct effect of DE exposure on hepatocytes was demonstrated by treatment of HepG2 cells with a

Corresponding author: Jesus A. Araujo, MD, PhD. Division of Cardiology, Department of Medicine, David Geffen School of Medicine, University of California-Los Angeles, 10833 Le Conte Avenue, CHS 43-264, Los Angeles, CA 90095. P.O. Box 951679. Phone number (310) 825-3222, Fax number (310) 206-9133. JAraujo@mednet.ucla.edu.

Disclosures:

Dr. Araujo, Dr. Rosenfeld and Dr. Lusis report grants from the National Institutes of Health, during the conduct of the study; no other conflict of interest is present.

methanol extract of DE particles followed by loading with oleic acid. As observed *in vivo*, this led to increased triglyceride content and significant downregulation of *ACAD9* mRNA expression. Treatment of HepG2 cells with DE particles and oleic acid did not alter *de-novo* lipogenesis, but inhibited total, mitochondrial and ATP-linked oxygen consumption rate, indicative of mitochondrial dysfunction. Treatment of isolated mitochondria, prepared from mouse liver, with DE particles and oleic acid also inhibited mitochondrial complex activity and β-oxidation.

Conclusions: Diesel exhaust exposure leads to dyslipidemia and liver steatosis in ApoE KO mice, likely due to mitochondrial dysfunction and decreased lipid catabolism.

Graphical Abstract

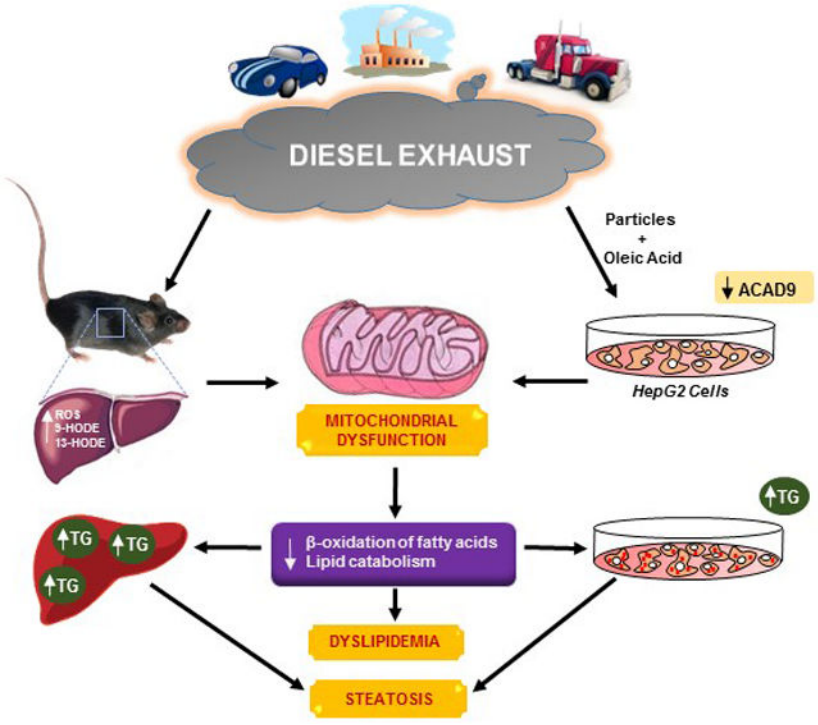

Keywords

Air Pollution; Liver Steatosis; Lipids; Triglycerides; Mitochondrial Dysfunction

Subject Codes:

Oxidative Stress; Lipids and Cholesterol; Metabolic Syndrome

Introduction

Exposure to air pollutants is associated with increased morbidity and mortality worldwide [1, 2]. Deaths are largely due to increased cardiovascular and cerebrovascular diseases of an ischemic nature [3], including acute coronary events, stroke and arrhythmias. These appear to occur in the setting of a common atherothrombotic substrate. While both particulate and

gaseous components have been associated with cardiovascular pathology, epidemiological studies show stronger associations with fine particulate matter (PM) with an aerodynamic diameter < 2.5 μm ($PM_{2.5}$) [1]. A large body of evidence, employing hyperlipidemic animal models, supports the causal link between PM exposure and atherosclerosis (reviewed by Araujo) [4].

We have reported that diesel exhaust (DE) emissions and ultrafine particles result in a pro-atherogenic lipid profile, consisting of LDL particles that are more oxidized (or prone to oxidation) and dysfunctional HDL, with decreased ability to protect against oxidation and inflammation [5-7]. Other studies have shown that PM exposure results in the induction of hyperlipidemia, alteration of lipid and carbohydrate metabolism resulting in insulin resistance, and non-alcoholic fatty liver disease (NAFLD) [8, 9]. NAFLD encompasses a wide spectrum of fatty degenerative disorders of the liver in the absence of alcohol intake, ranging from simple liver steatosis to steatohepatitis and cirrhosis [10]. NAFLD associates with metabolic syndrome and cardiovascular disease and its development could help to explain a portion of PM-induced cardiovascular morbidity and mortality [10]. Zheng et al reported that $PM_{2.5}$ exposures for 10 weeks lead to increased plasma levels of triglycerides and LDL/VLDL cholesterol, accompanied by triglyceride accumulation in the liver and the development of a non-alcoholic steatohepatitis (NASH)-like phenotype with fibrosis [8]. $PM_{2.5}$ in urban settings is enriched in particles from automobile engine emissions, which makes it likely that these particles could also be capable of inducing lipid dysregulatory actions. Therefore, it is critical to understand the mechanistic pathways by which PM induces dyslipidemia and lipid metabolic effects.

We have previously shown that a two week exposure to DE leads to increased lipid peroxidation in the lungs, blood and liver of ApoE KO mice, a mouse model which is prone to develop atherosclerotic lesions even when fed a normal laboratory diet [11]. However, we did not notice any effects on the quantitative levels of circulating plasma lipoproteins. We hypothesized that longer exposures were required to unveil effects on lipid metabolism that could influence levels of lipids in the blood. In the current study, we exposed ApoE KO mice to whole DE for 16 weeks to determine whether diesel emissions are capable of inducing effects on plasma and hepatic lipids.

Materials and Methods

The authors declare that all supporting data are available within the article [and its online supplementary files].

Exposure system

Characteristics of the exposure system have been previously described in details [12, 13]. Briefly, diesel exhaust (DE) was derived from a 5.5-kW, single-cylinder generator (Yanmar model YDG5500EV-6EI). We selected the engine load by setting a load bank (Simplex, Model Swift-E FT, Springfield, IL) to 4.0 kW ~ 72 % generator output. Ultra-low sulfur diesel fuel was used with a maximum sulfur content of 15 ppm, the present highway grade diesel fuel obtained from local fuel distributors. The generator lubricating oil was Chevron

DELO 400LE, SAE 15 W-40. All diluted air for the system was passed through HEPA and carbon filters, permitting a filtered air control exposure option with very low particulate and gaseous organic pollutant levels. The air entering the exposure room was conditioned to 18°C, and 60% relative humidity. During exposures, the concentrations of particulate were continuously measured and maintained at steady levels using a feedback controller monitoring fine particulate levels. Multi-stage samples that were collected on a micro-orifice uniform deposition impactor (MOUDI; MSP, Shoreview, MN) indicated a mass median diameter of 0.104 μm.

Lipoproteins and Carbohydrate metabolism

Plasma glucose concentrations were determined colorimetrically with the Glucose Trinder reagent (Sigma Diagnostics, St. Louis, MO) and insulin levels were determined with a sensitive insulin radioimmunoassay (RIA) kit (Linco Research, St. Charles, MO). HOMA-IR was calculated using the formula: HOMA-IR = [glucose (mg/dl) * insulin (m IU/mL)/ 22.5], using fasting values [14]. Plasma lipoprotein size fractions were determined by gel filtration chromatography as previously described [5]. For additional details, please refer to the supplemental material (avaiblable online at http://atvb.ahajournals.org).

Oxidized fatty acids

Mouse liver tissues were extracted and analyzed by LC-MS/MS as previously described [5], with minor modifications. Please refer to the online supplemental material for more details.

Tissue culture

Human hepatocellular carcinoma cell line HepG2 from American Type Culture Collection (ATCC, Manassas, VA, USA) was maintained as subconfluent monolayers in DMEM supplemented with 10% fetal bovine serum (Hyclone, Logan, UT) and 1% penicillin-streptomycin (Invitrogen, Carlsbad, CA). HepG2 cells were cultured at 37°C in a humidified atmosphere of 5% CO_2 and 95% air. The culture medium was changed every two days. In some experiments, HepG2 cells were treated with an organic extract of diesel exhaust particles (DEP), 50-100 μg/ml for 24-48 hours. DEP was obtained as a generous gift from Dr. Andrew Saxon at UCLA, originally generated at the National Institute of Environmental Studies (Tsukuba, Ibaraki, Japan). These particles were collected, characterized and underwent a methanol extraction as previously described [15].

Mitochondrial Bioenergetics

Oxygen consumption rate (OCR) was measured using a XF24 Analyzer (Agilent). For cellular OCR, HepG2 cells were incubated in unbuffered DMEM containing 25 mM glucose, 1 mM pyruvate and 2 mM glutamine. OCR was measured before (total respiration) and after the sequential injection of 0.75 μM oligomycin (complex V inhibitor), 0.2 μM carbonyl cyanide 4-(trifluoromethoxy)phenylhydrazone (FCCP, uncoupler), and 0.75 μM of rotenone and myxothiazol (complex I and III inhibitors, respectively), as described previously [16]. Mitochondrial respiration was calculated by subtracting the non-mitochondrial respiration left after rotenone and myxothiazol injection. Oligomycin-

sensitive respiration represents ATP-linked respiration (coupled respiration). To measure electron transport chain complex activity from cells, HepG2 cells were incubated in Mitochondrial Assay Solution (MAS) buffer with 10 mM pyruvate (complex I substrate), 2 mM malate, 4 μM FCCP, and 1 nM of XF Plasma Membrane Permeabilizer (PMP) reagent as previously described [17]. OCR was measured before and after the sequential injection of 2 μM rotenone, 10 mM succinate (complex II substrate), 4 μM antimycin A (complex III inhibitor), and a mix of 10 mM ascorbate and 100 μM TMPD (complex IV substrates), as described [17]. Antimycin A-sensitive respiration represents the complex III respiration. To measure OCR directly from mitochondria, mitochondria were isolated from fresh liver by dual centrifugation at 800g and 8000g [17]. Twelve μg of mitochondria were seeded per well by centrifugation. To assess β-oxidation, mitochondria were treated with 80 μM palmitoyl-carnitine/1 mM malate (fatty acid oxidation-driven complex I) in MAS buffer (without glucose) and vehicle, 1 mM OA and/or 100 μg/ml DEP for 1h at 37ºC. OCR was then measured before and after the sequential injections as described above. All data were normalized per μg of protein.

Gene expression

Total mRNA was harvested and gene expression levels were determined by quantitative PCR (qPCR) as previously described [6]. For additional details, please refer to the online supplemental material.

Statistical analyses

Data were reported as means ± SEM. Normality of data was assessed using the Shapiro-Wilk test (α=0.05), and homogeneity of variance was determined using either an F-test (for comparison of two groups) or Levene test (for comparison of three or more groups). Data were analyzed by parametric tests, unpaired Student's t test for comparison of two groups or One-way ANOVA followed by Tukey's post hoc test for comparison of three or more groups. If either normality or equal variance test failed, data were analyzed with non-parametric tests, Mann Whitney *U* test for comparison of two groups, or Kruskal Wallis test followed by Dunn's post hoc test for comparison of three or more groups. Associations between variables were determined by parametric linear regression analyses using Pearson correlation values, calculated with GraphPad Prism 6 software or RStudio 1.2.1335 for Windows. Statistical tests for each experiment were specified in the figure legends. *p* values < 0.05 were considered statistically significant.

Results

Exposure to diesel exhaust results in increased plasma and hepatic lipids

We exposed male ApoE KO mice, fed a normal laboratory diet, to DE vs. filtered air (FA) as controls for 16 weeks (Figure 1A). We noticed that DE-exposed mice exhibited higher plasma total cholesterol and triglyceride levels than FA-exposed controls (Table 1). Higher plasma cholesterol levels were due to cholesterol increases in the HDL and non-HDL fractions. FPLC profiles indicated increased cholesterol in particles from all fractions (VLDL, LDL+IDL and HDL) as evidenced by larger areas under the curve in each fraction

(Figure 1B). In addition, DE-exposed mice exhibited a VLDL fraction with a rightward shift as compared with FA controls, suggesting that VLDL particles could be smaller in DE-exposed mice (Figure 1B). Increases in triglyceride levels (Table 1) were due to increased triglyceride content of VLDL particles, but not in the other fractions, as judged by analyses of the FPLC profiles (Figure 1B). In contrast, hepatic cholesterol content was similar but DE-exposed mice showed a significant increase in hepatic triglyceride content as compared with FA controls (p=0.03) (Table 1), which suggested that either hepatic *de novo* lipogenesis (DNL), fatty acid uptake or lipid catabolism could be affected. Furthermore, DE also led to increased levels of 9-hydroxyoctadecadienoic (HODE) and 13-HODE acid in the liver (Figure 2A), derived from the oxidation of linoleic acid. Interestingly, there were associations between both 9-HODE and 13-HODE with triglyceride content (r= 0.5, Figure 2B), and although the correlations were not significant (p=0.08 and 0.09, respectively), they highly suggest that DE-induced oxidative stress could play a role in triglyceride accumulation in the liver.

Diesel exhaust dysregulates hepatic lipid catabolism.

To understand the mechanism responsible for DE-induced triglyceride accumulation in the liver, we assessed the mRNA expression levels of several genes known to be critical for hepatic DNL, including sterol regulatory element binding transcription factor (protein) 1c (*Srebp-1c*), fatty acid synthase (*Fasn*), stearoyl-CoA desaturase 1 (*Scd1*), fatty acid desaturase 6 (*Fads6*), diacylglyerol O-Acyltransferase 1 (*Dgat1*), and diacylglycerol O-Acyltransferase 2 (*Dgat2*). DE exposure did not lead to activation of lipogenic pathways or genes involved in translocation of fatty acids across the plasma membrane and fatty acid uptake such as solute carrier family 27 (fatty acid transporter) member 1 (*Slc27a1*). Instead, DE significantly downregulated ATP citrate lyase (*Acly*) (Figure 3A), suggesting that changes in hepatic *de novo* lipogenesis were not likely the primary cause of increased hepatic triglyceride accumulation.

We then explored whether DE affected lipid catabolism (Figure 3B). There was a decrease in the mRNA levels of peroxisome proliferator-activated receptor alpha (*Ppara*), a master regulator of fatty acid oxidation and homeostasis [18, 19] which did not reach statistical significance (p= 0.10). In addition, there was no difference in the protein levels of PPARα (Figure 3C) or *PPARα* target genes such as carnitine palmitoyltransferase 1 (*Cpt1) and 2* (*Cpt2)* (Figure 3B), vanin-1 (*Vnn1*), cytochrome P450 family 4 subfamily a polypeptide 14 (*Cyp4A14*) (Figure 3D), and instead, there was an increase in the mRNA levels of perilipin 5 (*Plin5*) (Figure 3D), also a PPARα target [20], indicating that the DE-induced elevation of hepatic triglycerides could not be ascribed to regulatory effects on PPARα. Importantly, there was a suggestive downregulation in the mRNA levels of acyl-coenzyme A dehydrogenase family member 9 (*Acad9*) (p= 0.08, Figure 3B), accompanied by an association between *Acad9* mRNA levels and liver triglycerides (Figure 3E) that was suggestive as well (p= 0.08). *Acad9* catalyzes the rate-limiting step in the β-oxidation of fatty acyl-CoA, and is specifically active toward palmitoyl-CoA and long-chain unsaturated substrates [21], suggesting that DE-induced steatosis could likely be due to decreased fatty acid catabolism.

HEPG2 cells also accumulate triglycerides after treatment with DEP

We explored whether the particulate component of DE had the ability to induce triglyceride accumulation in hepatocytes in culture, which would enable us to further dissect mediating pathways involved. HepG2 cells, treated with an organic extract of DE particles (DEP), 25-100 μg/ml for 24-48 hours, did not exhibit triglyceride accumulation (data not shown). We then treated HepG2 cells with 100 μg/ml DEP for 4 hours, followed by 2 mM oleic acid (OA) for 44 hours. Under these conditions, we noticed that DEP+OA resulted in significantly higher triglyceride accumulation than cells treated with only OA ($p<0.05$), DEP or media ($p<0.01$) (Figure 4A&B). We then asked whether an increase in triglyceride accumulation could be due to enhanced *de-novo* lipogenesis (DNL) in cells treated with DEP+OA. Thus, we assessed DNL using ^{14}[C] acetate in cells treated with DEP, OA, DEP +OA or media using the same conditions. Cells treated with DEP, OA or DEP+OA did not show higher DNL (Figure 4C), ruling out DNL as a key determinant of the triglyceride accumulation exhibited by cells treated with DEP+OA. Furthermore, there were no significant differences in mRNA levels of lipogenic genes *ACLY* and *ELOVL6* in DEP+OA treated cells as compared with OA-treated cells (Figure 4D), indicating that these enzymes were not involved in DEP-induced triglyceride accumulation in HepG2 cells. Although DEP +OA co-treatment led to a significant reduction in PPARα mRNA levels, expression of target genes *CPT1* and *VNN1* was unaffected or increased, indicating that DEP-induced triglyceride accumulation was not likely mediated by changes in PPARα expression (Figure 4E). Interestingly, however, DEP+OA co-treatment led to a significant decreased in the mRNA levels of *ACAD9* as compared with cells treated with OA only ($p= 0.01$, Figure 4E), consistent with similar effects *in vivo*.

DEP impairs mitochondrial function and lipid catabolism

ACAD9 deficiency has been reported to lead to defects in fatty acid β-oxidation and mitochondrial complex I deficiency [22, 23]. Therefore, we evaluated whether DEP exposure could induce mitochondrial dysfunction. HepG2 cells were treated with DEP, OA or DEP +OA as above. Oxygen consumption rate (OCR) was assessed by a Seahorse metabolic flux analyzer. Treatments with DEP and OA alone inhibited total OCR, which was due to a decrease in mitochondrial, and more precisely, ATP-linked respiration. Interestingly, co-treatment with DEP and OA inhibited mitochondrial respiration to a greater extent than DEP or OA treatments alone (Figure 5A&B). Using a plasma membrane permeabilizer reagent on HepG2 cells, we found that DEP significantly impaired mitochondrial complex I and IV activity when followed by OA treatment (DEP+OA, Figure 5C). Next, we asked whether DEP could directly affect the activity of isolated mitochondria. We prepared fresh mitochondria from mouse liver and treated them with 10 mM pyruvate/2 mM malate and 100 μg/ml DEP for 2 h in the absence or presence of 1 mM OA. Strikingly, DEP was able to impair mitochondrial respiration either by itself and/or together with OA, suggesting that the defect could be due in part to a direct effect of DEP on mitochondria (Figure 6A). We then evaluated if DEP-induced mitochondrial dysfunction could result in impaired β-oxidation. We treated fresh mitochondria with 100 μg/ml DEP +/− 1 mM OA for 1 hour, in the presence of 80 μM palmitoyl-carnitine/1 mM malate. Importantly, DEP+OA co-treatment markedly suppressed mitochondrial respiration driven by all complexes as compared with OA and/or media alone (Figure 6B), indicating an impairment in fatty acid oxidation and

supporting the notion that DEP-induced triglyceride accumulation was due to reduced lipid catabolism (Figure 7).

Discussion

This is the first report demonstrating effects of DE on lipid metabolism, liver steatosis, and mitochondrial functions. We found that ApoE KO mice fed a normal laboratory diet and exposed to whole DE for 16 weeks exhibited dyslipidemia and hepatic triglyceride accumulation (i.e. hepatic steatosis), likely due to mitochondrial dysfunction.

We have shown that exposure to ambient PM and DEP leads to enhanced atherosclerosis in ApoE KO mice [6, 24]. It has also been reported that C57BL/6 mice exposed to $PM_{2.5}$ for 10 weeks exhibited triglyceride accumulation and the development of a NASH-like phenotype [8], but pathogenic mechanisms remain unknown, as air pollution-induced liver steatosis is complex and likely to involve multiple pathways. We noted that 16-week exposure to DE led to increased hepatic triglyceride accumulation (Table 1), and that this was likely due to diminished lipid catabolism, rather than increased DNL. In addition, we noted that (human) HepG2 cells treated with DEP and exposed to fatty acids (OA) exhibited accumulated lipid and a significant downregulation of *ACAD9* ($p= 0.01$) (Figure 4E), which mediates β-oxidation of fatty acids in the mitochondria [21]. DEP, especially in the presence of OA, led to deficient cellular and mitochondrial respiration, indicative of mitochondrial dysfunction (Figure 5B). Furthermore, DEP+OA markedly suppressed β-oxidation as indicated by decreased respiration when fatty acids were the only source of energy but did not alter DNL. Consistent with our results, *ACAD9* mutations have been shown to induce mitochondrial dysfunction resulting in complex I deficiency, a mitochondrial respiratory chain disorder, with subsequent perturbation in transfer of electrons to coenzyme Q and downstream respiratory chain complexes [23]. However, DEP+OA suppressed other mitochondrial complexes besides complex I, which suggests the participation of additional mediating pathways.

We noted that DE exposure also resulted in markedly increased levels of 9- and 13-HODE indicating increased oxidative stress in the liver. 13-S-HODE has been reported to induce mitochondrial dysfunction as judged by alterations in calcium homeostasis and mitochondrial structural alterations in bronchial epithelial cells [25]. Although we did not assess the chiral distribution of increased 13-HODE, it is likely that the S steroisomer (13-S-HODE) was increased in DE-exposed livers as well by non-enzymatic and/or enzymatically mediated pathways, both of which lead to substantial oxidative conversion of linoleic acid into 13-S-HODE. Our results are consistent with the reported ability of DEP to induce $O_2^{\cdot -}$ generation, decrease of membrane potential, and loss of mitochondrial membrane mass in RAW 264.7 cells [26] as well as mitochondrial dysfunction in alveolar macrophages from mice exposed to DEP via pharyngeal aspiration [27]. Altogether, our in-vitro data strongly suggests that the DEP-induced triglyceride accumulation exhibited by live mice exposed to DE was likely due to mitochondrial dysfunction and suppressed fatty acid oxidation, either indirectly by increasing HODEs formation, and/or downregulating *Acad9,* or via direct interaction with the mitochondria (see proposed model in Figure 7). Future studies are being

directed at the 13-HODE/*Acad9*-mitochondrial dysfunction axis for understanding the effects of DE on hepatic physiology.

DE exposures also led to a suggestive downregulation of PPARα which could potentially mediate decreased β-oxidation of fatty acids and triglyceride accumulation in the liver in the same manner that PPARα KO mice exhibit decreased basal levels of β-oxidation of C16:0 [28] resulting in hepatic steatosis [29, 30]. However, not only decreased mRNA levels in DE-exposed mice did not reach statistical significance ($p= 0.10$) but also, there were neither differences in PPARα protein levels nor a consistent pattern of downregulation of PPARα target genes in livers from the DE group. Therefore, effects on PPARα are unlikely to explain the changes observed after 16 weeks of exposure to DE but we cannot rule out a potential role at earlier times of exposure. Thus, PPARα mRNA and protein levels have been reported to decrease in C57BL/6 mice exposed to $PM_{2.5}$ for 10 weeks [8]. In addition, we have noted that DEP-induced triglyceride synthesis in HepG2 cells was accompanied by decreased PPARα mRNA levels as well (Figure 4E), and it was completely abrogated by co-treatment with a PPARα activator (supplementary figure I), suggesting its potential value to mitigate PM-induced liver toxicity. Future studies with liver-specific PPARα KO mice will be needed to address whether regulation of PPARα plays any role in DE-induced liver steatotic effects.

The current study evaluates the effects of DE on ApoE KO mice fed a normal laboratory diet. This is a genetic model that shows a more modest degree of hepatic steatosis than either wild-type (WT) or ApoE KO mice challenged with a high fat diet [31-33]. ApoE KO mice exhibited marked hypercholesterolemia with either no [31] or modest increase [34] in the plasma levels of triglycerides, so it is important to note that DE exposure increased both plasma and hepatic levels of triglycerides together with increased hepatic levels of HODEs. 9-HODE [35] and 13-HODE [35, 36] have been found significantly elevated in patients with NASH (grade II steatosis) compared with patients with simple steatosis (grade I steatosis) or normal liver biopsies [36]. 9-HODE, in particular, plays an important role in the inflammatory process by regulating monocyte and macrophage functions [37]. However, in spite of a significant increase in 9-HODE, DE led to a modest development of hepatic steatosis without obvious histological evidence of inflammation or fibrosis (supplementary figure II). These effects were more modest than those induced by 10-week exposures to $PM_{2.5}$ on C57BL/6 mice fed a normal laboratory or a high fat diet [8, 38]. One possibility is that longer exposures would have been required to develop steatohepatitis. Another possibility is that lack of inflammation could have been due to the concurrent increased levels of 13-HODE which may have inhibited the proinflammatory activity of 9-HODE, in a similar manner how 13-HODE inhibits the exacerbation of an inflammatory response induced by 9-HODE in RAW264.7 macrophages stimulated with LPS [39]. Alternatively, this could have been due to differences between DE and $PM_{2.5}$ toxicity, the different mouse models employed or other experimental factors.

DE exposure for 16 weeks led to hypertriglyceridemia and hypercholesterolemia. $PM_{2.5}$ exposures have also been reported to increase plasma levels of triglycerides accompanied by increased LDL/VLDL cholesterol ratios and insulin resistance but without altering HDL or total plasma cholesterol levels [8]. On the contrary, we observed increased cholesterol in all

fractions and triglycerides in the VLDL fraction (Figure 1), without evidence for insulin resistance (supplementary figure III). Although the current study did not investigate precise mechanisms involved in the alteration of cholesterol homeostasis, it is unlikely that these effects were due to increased hepatic cholesterol synthesis. DE did not upregulate the mRNA expression levels of various enzymes involved in critical steps of cholesterol biosynthesis such as 3-hydroxy-3-methylglutaryl-CoA reductase (*Hmgcr)*, mevalonate diphosphate decarboxylase (*Mvd*) or squalene epoxidase (*Sqle*). Instead, DE led to decreased levels of *Mvd* (supplementary figure IV). It is likely that DE influenced other cholesterol metabolic pathways, a possibility that will need to be addressed by future studies. On the other hand, there were trends for correlations between plasma triglycerides, and liver 9-HODE (r=0.56), 13-HODE (r=0.53) and triglycerides (r= 0.324, supplementary figure V), suggesting that DE effects on plasma triglycerides could be related to increased hepatic VLDL production. However, given the systemic nature of DE exposures, it is also possible that other mechanisms involving lipid uptake by the liver, intestinal lipid absorption, or changes in peripheral tissues (e.g., adipose tissue, muscle) could have contributed to the DE-induced lipid metabolic effects (Figure 7). Future studies will also need to address these various possibilities.

How does inhalation of DE induce these metabolic effects in tissues system-wide? One possibility is that inhaled DEP are translocated systemically to the liver. It has been reported that Kupffer cells might take up particles after inhalation of concentrated $PM_{2.5}$ [40] but particles have yet to be identified in hepatocytes. It is also possible that chemical constituents leach from lung-inhaled DEP and are subsequently transported to the liver via the systemic circulation. A third possibility is that DEP gain access to the gastrointestinal (GI) tract, considering that inhaled particles can enter the GI tract as a result of rapid bronchial mucocilliary cleansing to the oropharynx, followed by swallowing [41]. Alternatively, semivolatile organic compounds (SVOC) present in inhaled particles could volatilize and access the GI tract in the gaseous phase. Therefore, particulate and/or gaseous components could access and exert biological effects in the GI tract, and possibly be absorbed into the enterohepatic and systemic circulation. Indeed, we have previously reported that *Ldlr* KO mice exposed to inhaled ambient ultrafine particles for 10 weeks developed intestinal inflammation together with increased intestinal and plasma levels of 9-HODE [42, 43].

In summary, chronic exposure to DE causes increased plasma levels of triglycerides and cholesterol as well as hepatic steatosis, which are all hallmark components of the metabolic syndrome. Our data strongly suggest that the effects are due to, at least in part, decreased lipid catabolism in the liver likely due to mitochondrial dysfunction. Although DE emissions have a high content of particles in the ultrafine-size range with a particle size distribution similar to our previous studies [5], it is still to be determined which component(s) of DE are responsible for the observed effects.

Supplementary Material

Refer to Web version on PubMed Central for supplementary material.

Acknowledgements

We are grateful to Andrew Saxon who generously provided the DEP, Sarada Charugundla for determining plasma insulin and glucose levels, and Peter Tontonoz for his thoughtful advice on the metabolic studies.

Sources of Funding:

This work was supported by the National Institute of Environmental Health Sciences, National Institutes of Health (ONES RO1 Award ES016959, R56 ES016959-06 and R01ES029395 to JAA as well as P50 ES015915 to MER in the DISCOVER Center [J. Kaufman PI]), the American Heart Association (15POST22150008 to WSD), and the National Heart, Lung, and Blood Institute (R01 HL28481 to AJL).

Abbreviations:

ApoE KO	Apolipoprotein E Knockout
DE	Diesel Exhaust
DEP	Diesel exhaust particles
DNL	De novo lipogenesis
FA	Filtered air
HDL	High density lipoproteins
LPS	Lipopolysacharide
LDL	Low density lipoproteins
NAFLD	Non-alcoholic fatty liver disease
NASH	Non-alcoholic steatohepatitis
OA	Oleic acid
PM	Particulate matter
SVOC	semivolatile organic compounds
VLDL	Very low density lipoproteins
WT	wild-type

References

1. Brook RD, Rajagopalan S, Pope CA, III, et al. Particulate matter air pollution and cardiovascular disease. An update to the scientific statement from the american heart association. Circulation. 2010:CIR.0b013e3181dbece3181
2. World Health Organization. Burden of disease from ambient air pollution for 2012. 2014
3. Pope CA, 3rd, Burnett RT, Thurston GD, Thun MJ, Calle EE, Krewski D, Godleski JJ. Cardiovascular mortality and long-term exposure to particulate air pollution: Epidemiological evidence of general pathophysiological pathways of disease. Circulation. 2004;109:71–77 [PubMed: 14676145]
4. Araujo J Particulate air pollution, systemic oxidative stress, inflammation, and atherosclerosis. Air Quality, Atmosphere & Health. 2011;4:79–93

5. Yin F, Lawal A, Ricks J, Fox JR, Larson T, Navab M, Fogelman AM, Rosenfeld ME, Araujo JA. Diesel exhaust induces systemic lipid peroxidation and development of dysfunctional pro-oxidant and pro-inflammatory high-density lipoprotein. Arteriosclerosis, Thrombosis, and Vascular Biology. 2013;33:1153–1161
6. Araujo JA, Barajas B, Kleinman M, Wang X, Bennett BJ, Gong KW, Navab M, Harkema J, Sioutas C, Lusis AJ, Nel AE. Ambient particulate pollutants in the ultrafine range promote early atherosclerosis and systemic oxidative stress. Circ Res. 2008;102:589–596 [PubMed: 18202315]
7. Li R, Navab M, Pakbin P, Ning Z, Navab K, Hough G, Morgan TE, Finch CE, Araujo JA, Fogelman AM, Sioutas C, Hsiai T. Ambient ultrafine particles alter lipid metabolism and hdl anti-oxidant capacity in ldlr-null mice. Journal of Lipid Research. 2013;54:1608–1615 [PubMed: 23564731]
8. Zheng Z, Xu X, Zhang X, Wang A, Zhang C, Huttemann M, Grossman LI, Chen LC, Rajagopalan S, Sun Q, Zhang K. Exposure to ambient particulate matter induces a nash-like phenotype and impairs hepatic glucose metabolism in an animal model. Journal of hepatology. 2013;58:148–154 [PubMed: 22902548]
9. Sun Q, Yue P, Deiuliis JA, Lumeng CN, Kampfrath T, Mikolaj MB, Cai Y, Ostrowski MC, Lu B, Parthasarathy S, Brook RD, Moffatt-Bruce SD, Chen LC, Rajagopalan S. Ambient air pollution exaggerates adipose inflammation and insulin resistance in a mouse model of diet-induced obesity. Circulation. 2009;119:538–546 [PubMed: 19153269]
10. Byrne CD, Olufadi R, Bruce KD, Cagampang FR, Ahmed MH. Metabolic disturbances in non-alcoholic fatty liver disease. Clin Sci (Lond). 2009;116:539–564 [PubMed: 19243311]
11. Barajas B, Che N, Yin F, Rowshanrad A, Orozco LD, Gong KW, Wang X, Castellani LW, Reue K, Lusis AJ, Araujo JA. Nf-e2-related factor 2 promotes atherosclerosis by effects on plasma lipoproteins and cholesterol transport that overshadow antioxidant protection. Arterioscler Thromb Vasc Biol. 2011;31:58–66 [PubMed: 20947826]
12. Fox JR, Cox DP, Drury BE, Gould TR, Kavanagh TJ, Paulsen MH, Sheppard L, Simpson CD, Stewart JA, Larson TV, Kaufman JD. Chemical characterization and in vitro toxicity of diesel exhaust particulate matter generated under varying conditions. Air Qual Atmos Health. 2015;8:507–519 [PubMed: 26539254]
13. Gould T, Larson T, Stewart J, Kaufman JD, Slater D, McEwen N. A controlled inhalation diesel exhaust exposure facility with dynamic feedback control of pm concentration. Inhal Toxicol. 2008;20:49–52 [PubMed: 18236222]
14. Matthews DR, Hosker JP, Rudenski AS, Naylor BA, Treacher DF, Turner RC. Homeostasis model assessment: Insulin resistance and beta-cell function from fasting plasma glucose and insulin concentrations in man. Diabetologia. 1985;28:412–419 [PubMed: 3899825]
15. Lawal AO, Zhang M, Dittmar M, Lulla A, Araujo JA. Heme oxygenase-1 protects endothelial cells from the toxicity of air pollutant chemicals. Toxicol Appl Pharmacol. 2015;284:281–291 [PubMed: 25620054]
16. Wu M, Neilson A, Swift AL, Moran R, Tamagnine J, Parslow D, Armistead S, Lemire K, Orrell J, Teich J, Chomicz S, Ferrick DA. Multiparameter metabolic analysis reveals a close link between attenuated mitochondrial bioenergetic function and enhanced glycolysis dependency in human tumor cells. Am J Physiol Cell Physiol. 2007;292:C125–136 [PubMed: 16971499]
17. Rogers GW, Brand MD, Petrosyan S, Ashok D, Elorza AA, Ferrick DA, Murphy AN. High throughput microplate respiratory measurements using minimal quantities of isolated mitochondria. PLoS One. 2011;6:e21746 [PubMed: 21799747]
18. Desvergne B, Wahli W. Peroxisome proliferator-activated receptors: Nuclear control of metabolism. Endocr Rev. 1999;20:649–688 [PubMed: 10529898]
19. Leone TC, Weinheimer CJ, Kelly DP. A critical role for the peroxisome proliferator-activated receptor alpha (pparalpha) in the cellular fasting response: The pparalpha-null mouse as a model of fatty acid oxidation disorders. Proc Natl Acad Sci U S A. 1999;96:7473–7478 [PubMed: 10377439]
20. Dalen KT, Dahl T, Holter E, Arntsen B, Londos C, Sztalryd C, Nebb HI. Lsdp5 is a pat protein specifically expressed in fatty acid oxidizing tissues. Biochim Biophys Acta. 2007;1771:210–227 [PubMed: 17234449]

21. Zhang J, Zhang W, Zou D, Chen G, Wan T, Zhang M, Cao X. Cloning and functional characterization of acad-9, a novel member of human acyl-coa dehydrogenase family. Biochem Biophys Res Commun. 2002;297:1033–1042 [PubMed: 12359260]
22. Leipnitz G, Mohsen AW, Karunanidhi A, Seminotti B, Roginskaya VY, Markantone DM, Grings M, Mihalik SJ, Wipf P, Van Houten B, Vockley J. Evaluation of mitochondrial bioenergetics, dynamics, endoplasmic reticulum-mitochondria crosstalk, and reactive oxygen species in fibroblasts from patients with complex i deficiency. Sci Rep. 2018;8:1165 [PubMed: 29348607]
23. Haack TB, Danhauser K, Haberberger B, et al. Exome sequencing identifies acad9 mutations as a cause of complex i deficiency. Nat Genet. 2010;42:1131–1134 [PubMed: 21057504]
24. Miller MR, McLean SG, Duffin R, Lawal AO, Araujo JA, Shaw CA, Mills NL, Donaldson K, Newby DE, Hadoke PW. Diesel exhaust particulate increases the size and complexity of lesions in atherosclerotic mice. Part Fibre Toxicol. 2013;10:61 [PubMed: 24330719]
25. Mabalirajan U, Rehman R, Ahmad T, Kumar S, Singh S, Leishangthem GD, Aich J, Kumar M, Khanna K, Singh VP, Dinda AK, Biswal S, Agrawal A, Ghosh B. Linoleic acid metabolite drives severe asthma by causing airway epithelial injury. Sci Rep. 2013;3:1349 [PubMed: 23443229]
26. Xia T, Korge P, Weiss JN, Li N, Venkatesen MI, Sioutas C, Nel A. Quinones and aromatic chemical compounds in particulate matter induce mitochondrial dysfunction: Implications for ultrafine particle toxicity. Environ Health Perspect. 2004;112:1347–1358 [PubMed: 15471724]
27. Zhao H, Ma JK, Barger MW, Mercer RR, Millecchia L, Schwegler-Berry D, Castranova V, Ma JY. Reactive oxygen species- and nitric oxide-mediated lung inflammation and mitochondrial dysfunction in wild-type and inos-deficient mice exposed to diesel exhaust particles. J Toxicol Environ Health A. 2009;72:560–570 [PubMed: 19267316]
28. Aoyama T, Peters JM, Iritani N, Nakajima T, Furihata K, Hashimoto T, Gonzalez FJ. Altered constitutive expression of fatty acid-metabolizing enzymes in mice lacking the peroxisome proliferator-activated receptor alpha (pparalpha). J Biol Chem. 1998;273:5678–5684 [PubMed: 9488698]
29. Blavy P, Gondret F, Guillou H, Lagarrigue S, Martin PG, van Milgen J, Radulescu O, Siegel A. A minimal model for hepatic fatty acid balance during fasting: Application to ppar alpha-deficient mice. J Theor Biol. 2009;261:266–278 [PubMed: 19635486]
30. Abdelmegeed MA, Moon KH, Hardwick JP, Gonzalez FJ, Song BJ. Role of peroxisome proliferator-activated receptor-alpha in fasting-mediated oxidative stress. Free Radic Biol Med. 2009;47:767–778 [PubMed: 19539749]
31. Ferre N, Martinez-Clemente M, Lopez-Parra M, Gonzalez-Periz A, Horrillo R, Planaguma A, Camps J, Joven J, Tres A, Guardiola F, Bataller R, Arroyo V, Claria J. Increased susceptibility to exacerbated liver injury in hypercholesterolemic apoe-deficient mice: Potential involvement of oxysterols. Am J Physiol Gastrointest Liver Physiol. 2009;296:G553–562 [PubMed: 19136384]
32. Smith DD, Tan X, Raveendran VV, Tawfik O, Stechschulte DJ, Dileepan KN. Mast cell deficiency attenuates progression of atherosclerosis and hepatic steatosis in apolipoprotein e-null mice. Am J Physiol Heart Circ Physiol. 2012;302:H2612–2621 [PubMed: 22505639]
33. Stachowicz A, Olszanecki R, Suski M, Wisniewska A, Toton-Zuranska J, Madej J, Jawien J, Bialas M, Okon K, Gajda M, Glombik K, Basta-Kaim A, Korbut R. Mitochondrial aldehyde dehydrogenase activation by alda-1 inhibits atherosclerosis and attenuates hepatic steatosis in apolipoprotein e-knockout mice. J Am Heart Assoc. 2014;3:e001329 [PubMed: 25392542]
34. Zhang SH, Reddick RL, Piedrahita JA, Maeda N. Spontaneous hypercholesterolemia and arterial lesions in mice lacking apolipoprotein e. Science. 1992;258:468–471 [PubMed: 1411543]
35. Maciejewska D, Ossowski P, Drozd A, Ryterska K, Jamiol-Milc D, Banaszczak M, Kaczorowska M, Sabinicz A, Raszeja-Wyszomirska J, Stachowska E. Metabolites of arachidonic acid and linoleic acid in early stages of non-alcoholic fatty liver disease--a pilot study. Prostaglandins Other Lipid Mediat. 2015;121:184–189 [PubMed: 26408952]
36. Feldstein AE, Lopez R, Tamimi TA, Yerian L, Chung YM, Berk M, Zhang R, McIntyre TM, Hazen SL. Mass spectrometric profiling of oxidized lipid products in human nonalcoholic fatty liver disease and nonalcoholic steatohepatitis. J Lipid Res. 2010;51:3046–3054 [PubMed: 20631297]

37. Vangaveti V, Baune BT, Kennedy RL. Hydroxyoctadecadienoic acids: Novel regulators of macrophage differentiation and atherogenesis. Ther Adv Endocrinol Metab. 2010;1:51–60 [PubMed: 23148150]

38. Zheng Z, Zhang X, Wang J, Dandekar A, Kim H, Qiu Y, Xu X, Cui Y, Wang A, Chen LC, Rajagopalan S, Sun Q, Zhang K. Exposure to fine airborne particulate matters induces hepatic fibrosis in murine models. Journal of hepatology. 2015;63:1397–1404 [PubMed: 26220751]

39. Warner DR, Liu H, Miller ME, Ramsden CE, Gao B, Feldstein AE, Schuster S, McClain CJ, Kirpich IA. Dietary linoleic acid and its oxidized metabolites exacerbate liver injury caused by ethanol via induction of hepatic proinflammatory response in mice. Am J Pathol. 2017;187:2232–2245 [PubMed: 28923202]

40. Tan HH, Fiel MI, Sun Q, Guo J, Gordon RE, Chen LC, Friedman SL, Odin JA, Allina J. Kupffer cell activation by ambient air particulate matter exposure may exacerbate non-alcoholic fatty liver disease. J Immunotoxicol. 2009;6:266–275 [PubMed: 19908945]

41. Moller W, Haussinger K, Winkler-Heil R, Stahlhofen W, Meyer T, Hofmann W, Heyder J. Mucociliary and long-term particle clearance in the airways of healthy nonsmoker subjects. J Appl Physiol. 2004;97:2200–2206 [PubMed: 15347631]

42. Li R, Mittelstein D, Kam W, Pakbin P, Du Y, Tintut Y, Navab M, Sioutas C, Hsiai T. Atmospheric ultrafine particles promote vascular calcification via the nf-kappab signaling pathway. Am J Physiol Cell Physiol. 2013;304:C362–369 [PubMed: 23242187]

43. Li R, Navab K, Hough G, et al. Effect of exposure to atmospheric ultrafine particles on production of free fatty acids and lipid metabolites in the mouse small intestine. Environ Health Perspect. 2015;123:34–41 [PubMed: 25170928]

Highlights:

- Diesel Exhaust Induces Hypertriglyceridemia and Hypercholesterolemia
- Diesel exhaust alters lipid and carbohydrate metabolism
- Diesel exhaust induces liver steatosis, likely due to decreased lipid catabolism
- Development of hepatic steatosis is likely due to mitochondrial dysfunction in the liver.

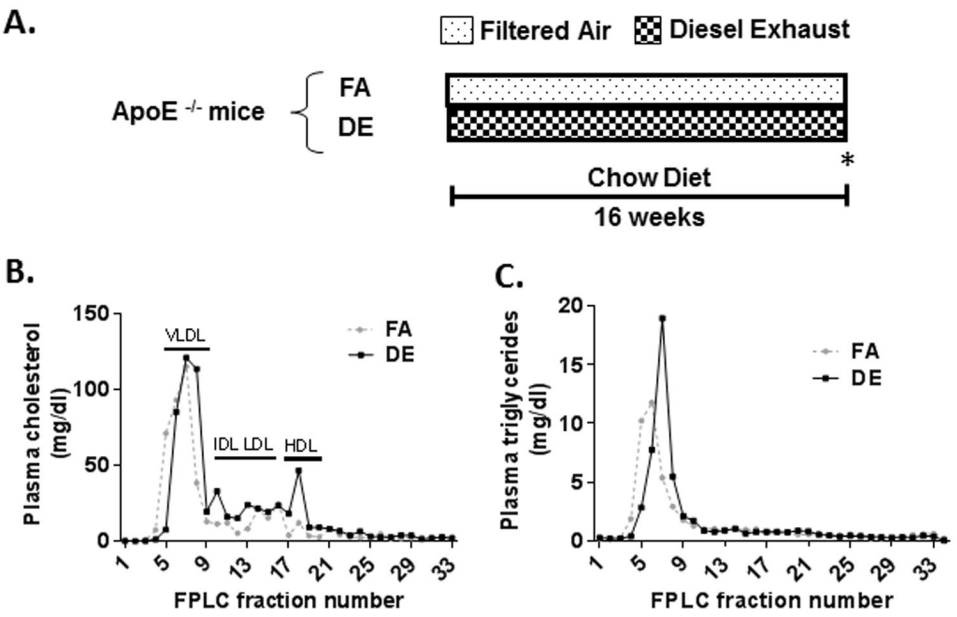

Figure 1. Diesel exhaust exposures influence plasma lipoproteins.

(A) Experimental protocol. Two groups of male ApoE KO mice were exposed to filtered air (FA) or diesel exhaust (DE) for 16 weeks. *Time at which mice were bled, euthanized and tissue harvesting performed. (B&C) FPLC profiles for plasma cholesterol (B) and plasma triglycerides (C) using pools of plasma.

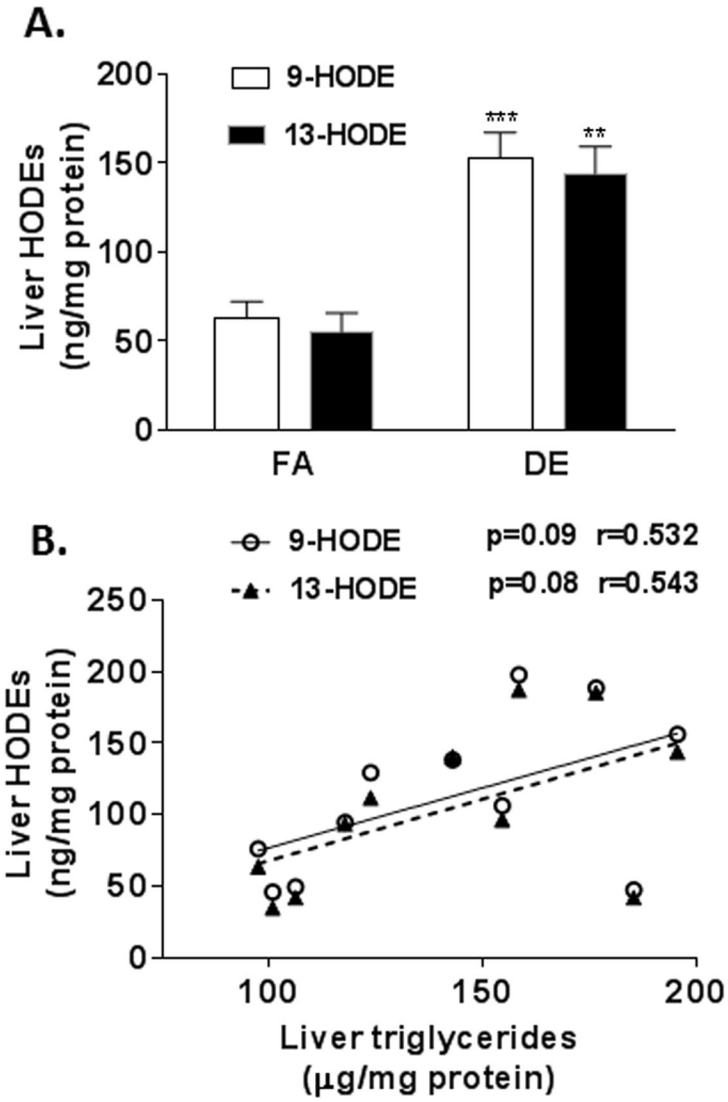

Figure 2. Diesel exhaust induces systemic oxidative stress and liver steatosis.

(A) Mouse liver HODEs in mice exposed to filtered air (FA) vs. diesel exhaust (DE) for 16 weeks, determined by mass spectrometry. Each bar denotes mean ± SEM (n=8). (B) Correlation between liver triglycerides and liver HODEs. Triglycerides were determined with an enzymatic colorimetric method. **p<0.01, ***p<0.001 DE vs. FA controls using unpaired Student's t test.

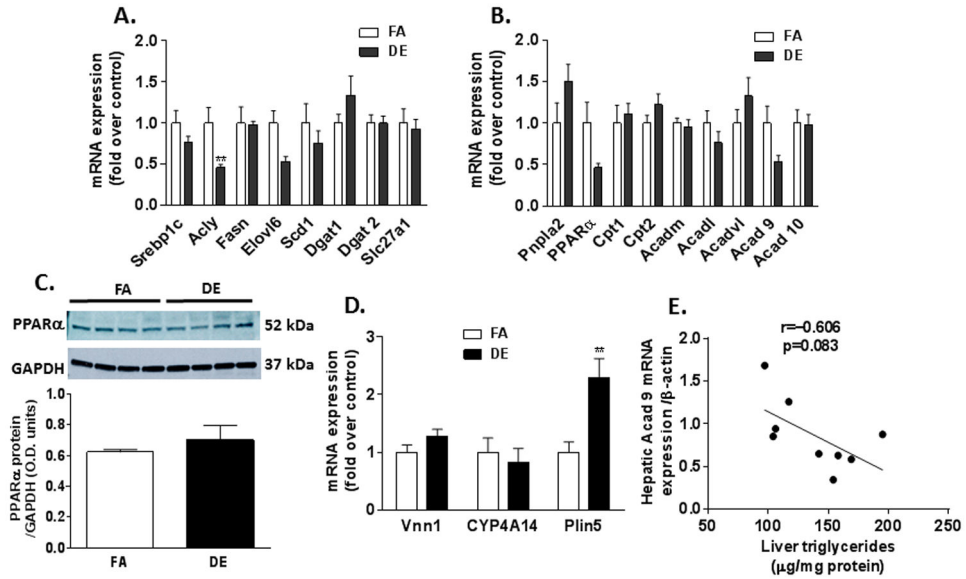

Figure 3. Diesel exhaust and lipid metabolic genes.

Quantitative PCR analysis of (A) Fatty acid and triglyceride synthesis-related genes, (B) Mitochondrial transport and fatty acid oxidation-related genes in liver. (C) Immunoblotting analysis of PPARα protein expression in the liver. (D) Additional PPARα target genes in liver. (E) Correlation between levels of liver triglycerides and hepatic Acad 9 mRNA expression. Each bar denotes mean ± SEM (n= 8 for mRNA expression; n=4 for immunoblot), **p<0.01 DE vs. FA controls using Mann Whitney test.

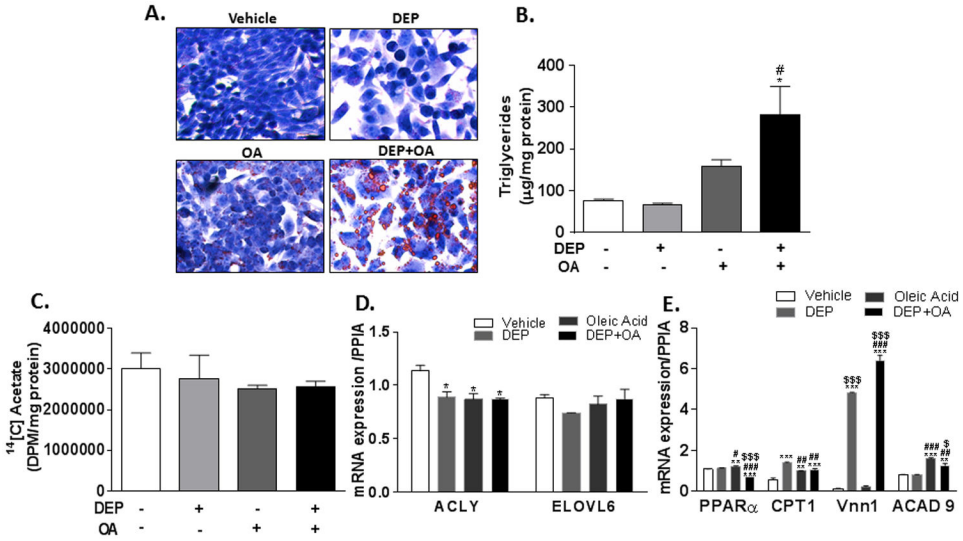

Figure 4. Diesel exhaust particles and triglyceride accumulation in HepG2 cells.

HepG2 cells were treated with 100 µg/ml DEP, 2 mM oleic acid (OA), vehicle control for 48 h, or 100 µg/ml DEP for 4h, followed by 2 mM oleic acid for 44 h (DEP+OA). (A) Representative photomicrographs of HepG2 cells stained with Oil Red O, (B) Content of triglycerides in the cells, (C) *De-novo* lipogenesis in cells with ^{14}[C] acetate incorporation into total lipids, (D) mRNA expression levels of lipogenic genes, and (E) fatty acid-oxidation genes, *p<0.05, **p<0.01, ***p<0.001 vs vehicle control, # p<0.05, ## p<0.01, ### p<0.001 vs DEP treatment, and $ p<0.05, $ $ $ p<0.001 vs OA treatment, using One-way ANOVA and Tukey's post-hoc test. DPM=Disintegrations per minute.

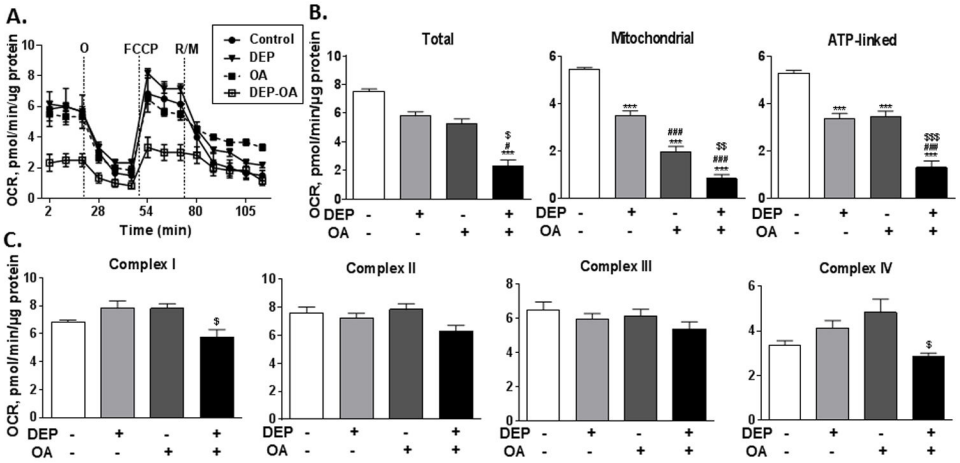

Figure 5. Cellular and mitochondrial respiration.

HepG2 cells were treated with 100 μg/ml DEP, 2 mM oleic acid (OA), vehicle control for 48 h, or 100 μg/ml DEP for 4h, followed by 2 mM oleic acid for 44 h (DEP+OA). (A) Oxygen consumption rate (OCR) was measured before and after the sequential injections of 0.75 μM oligomycin (O), 0.2 μM carbonyl cyanide 4-(trifluoromethoxy)phenylhydrazone (FCCP) and 0.75 μM of rotenone and myxothiazol (R/M). (B) Total, mitochondrial and ATP-linked respiration. (C) Mitochondrial respiration of complexes I to IV. *p<0.05, **p<0.01, ***p<0.001 vs vehicle control, # p<0.05, ### p<0.001 vs DEP treatment, $ p<0.05, $ $ p<0.01, $ $ $ p<0.001 vs OA treatment, analyzed using One-way ANOVA and Tukey's post-hoc test except Total respiration in panel B and complex I respiration in panel C, which were analyzed by Kruskal-Wallis test followed by Dunn's post-hoc test with Benjamini-Hochberg correction.

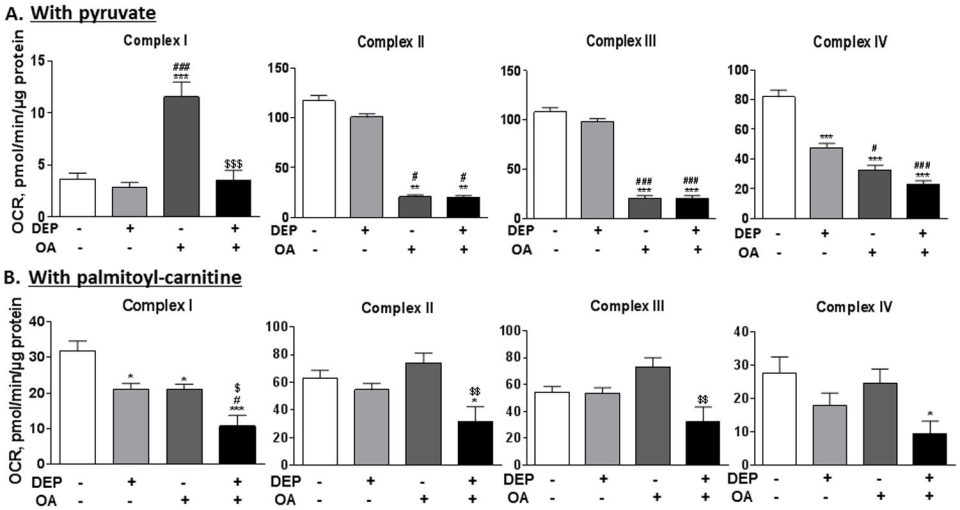

Figure 6. Diesel exhaust induces mitochondrial dysfunction.

Mitochondrial complexes I-IV oxygen consumption rate (OCR) was measured in mitochondria isolated from mouse liver with vehicle, 100 μg/ml DEP, 2 mM oleic acid (OA) or DEP and OA in combination, using (A) pyruvate after 2h treatment and (B) palmitoyl-carnitine after 1h treatment as described in the methods. *p<0.05, **p<0.01, ***p<0.001 vs vehicle control, # p<0.05, ## p<0.01, ### p<0.001 vs DEP treatment, $ p<0.05, $ $ p<0.01, $ $ $ p<0.001 vs OA treatment, analyzed using One-way ANOVA and Tukey's post-hoc test except Complex II respiration in panel A, which was analyzed by Kruskal-Wallis test followed by Dunn's post-hoc test with Benjamini-Hochberg correction.

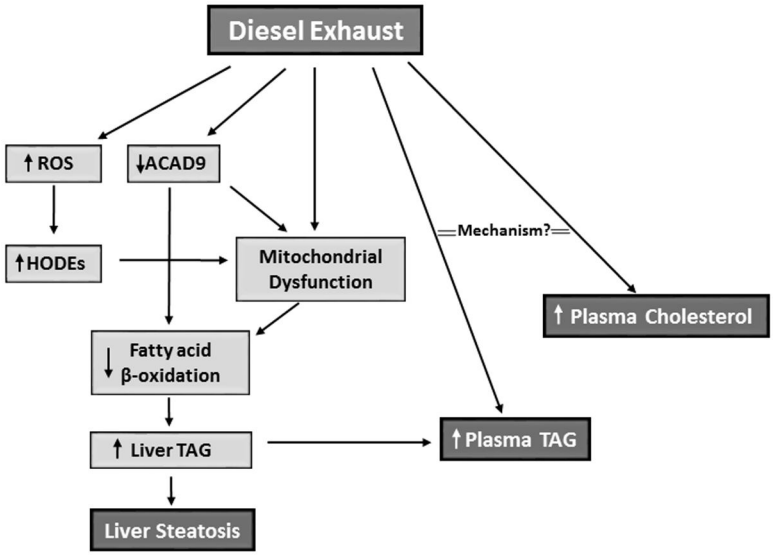

Figure 7. Schematic diagram.

Proposed model of DE-induced hyperlipidemia, liver steatosis and mitochondrial dysfunction. ROS= Reactive Oxygen Species, TAG= Triglycerides.

Table 1.

Levels of plasma and hepatic lipids[a]

	FA	DE	p
Plasma			
Total cholesterol (mg/dl) [b]	453.4±27.9	615.8±15.3	<0.0001
HDL cholesterol (mg/dl) [c]	46.5±2.7	60.9±4.8	<0.05
Non HDL cholesterol (mg/dl) [c]	386.8±15.9	566.51±13.4	<0.0001
Total cholesterol/HDL cholesterol [c]	11.0±1.1	13.4±1.4	0.2
Triglycerides (mg/dl) [b]	71.9±6.9	93.4±5.6	<0.05
Liver			
Cholesterol (μg/mg protein) [b]	15.9±1.1	15.2±0.5	0.6
Triglycerides (μg/mg protein) [b]	122.0±10.6	155.1±9.1	<0.05

[a] Results are expressed as mean ± SEM.

[b] n=8 for each group.

[c] n=7 for FA group, n=8 for DE group.